Inhibition of Dexamethasone-induced Fatty Liver Development by Reducing miR-17-5p Levels

William W Du[1,2], Fengqiong Liu[1–3], Sze Wan Shan[1,2], Xindi Cindy Ma[1,2], Shaan Gupta[1,2], Tianru Jin[4], David Spaner[1], Sergey N Krylov[5], Yaou Zhang[6], Wenhua Ling[3] and Burton B Yang[1,2]

[1]Sunnybrook Research Institute, Sunnybrook Health Sciences Centre, Toronto, Ontario, Canada; [2]Department of Laboratory Medicine and Pathobiology, University of Toronto, Toronto, Ontario, Canada; [3]School of Public Health, Sun Yat-sen University, Guangzhou, P.R. China; [4]Toronto General Research Institute, University Health Network, Toronto, Ontario, Canada; [5]Department of Chemistry and Centre for Research on Biomolecular Interactions, York University, Toronto, Ontario, Canada; [6]Key Lab in Healthy Science and Technology, Division of Life Science, Graduate School at Shenzhen, Tsinghua University, Shenzhen, P.R. China

Steatosis is a pivotal event in the initiation and progression of nonalcoholic fatty liver disease (NAFLD) which can be driven by peroxisome proliferator-activated receptor-α (PPAR-α) dysregulation. Through examining the effect of PPAR-α on fatty liver development, we found that PPAR-α is a target of miR-17-5p. Transgenic mice expressing miR-17 developed fatty liver and produced higher levels of triglyceride and cholesterol but lower levels of PPAR-α. Ectopic expression of miR-17 enhanced cellular steatosis. Gain-of-function and loss-of-function experiments confirmed PPAR-α as a target of miR-17-5p. On the other hand, PPAR-α bound to the promoter of miR-17 and promoted its expression. The feed-back loop between miR-17-5p and PPAR-α played a key role in the induction of steatosis and fatty liver development. Mice with high levels of miR-17-5p were sensitive to Dexamethasone-induced fatty liver formation. Inhibition of miR-17-5p suppressed this process and enhanced PPAR-α expression in mice treated with Dexamethasone. Clofibrate, Ciprofibrate, and WY-14643: three agents used for treatment of metabolic disorders, were found to promote PPAR-α expression while decreasing miR-17-5p levels and inhibiting steatosis. Our studies show that miR-17-5p inhibitor and agents used in metabolic disorders may be applied in combination with Dexamethasone in the treatment of anti-inflammation, immunosuppression, and cancer patients.

Received 2 November 2014; accepted 27 March 2015; advance online publication 19 May 2015. doi:10.1038/mt.2015.64

INTRODUCTION

Nonalcoholic fatty liver disease (NAFLD) represents a spectrum of metabolic syndrome-associated liver disease progressing from simple steatosis, through nonalcoholic steatohepatitis (NASH) and fibrosis to cirrhosis and hepatocellular carcinoma.[1,2] While its risk factors have been clearly defined, the underlying mechanisms of the disease progression remain poorly understood. Although the general pathogenesis includes insulin resistance, oxidative stress, inflammation, hepatocyte injury, cellular apoptosis, fibrosis, and carcinogenesis, steatosis is the very initial and vital step in the progress of NAFLD.[2,3]

Glucocorticoids are a class of steroid used extensively for anti-inflammation in patients with allergies, asthma, autoimmune diseases, sepsis, and cancers. They are also used for patients with metabolic disorders. The side-effects include hyperglycemia due to increased insulin resistance and impaired glucose tolerance, leading to the development of steatosis and fatty liver.[4] One of the most popular used drugs in this class of steroids is Dexamethasone (DXM), which is 25 times more potent than cortisol in its glucocorticoid effect.

Peroxisome proliferator-activated receptor-α (PPAR-α) is a nuclear receptor protein encoded by the *PPARA* gene.[5] It serves as a transcription factor and a major regulator of lipid metabolism in the liver, which is activated under nutrient-deficient conditions.[6] Increased expression of PPAR-α promotes uptake, utilization, and catabolism of fatty acids. Upregulation of PPAR-α is dependent on the presence of fatty acid synthase.[7] PPAR-α is a ligand-activated transcriptional factor that can bind to specific PPAR-response elements of certain genes with its heterodimeric partner retinoid X for regulatory purposes,[8] thus playing a crucial role in intracellular lipid metabolism. Previous reports demonstrated that PPAR-α exerted its role in hepatic lipid metabolism through activating genes involved with fatty acid β-oxidation,[9] leading to upregulation of malonyl-CoA decarboxylase to increase translocation of fatty acids into mitochondria for oxidation,[10,11] and lowering the hepatic substrate for triglyceride synthesis by limiting its output from other organs.[11] Furthermore, PPAR-α reduces *de novo* fatty acid synthesis by blocking enzymes like acetyl-CoA carboxylase and fatty acid synthase.[9]

MicroRNAs (miRNAs) are small noncoding RNAs that negatively regulate target gene expression through partial base pairing with 3' untranslated regions (UTRs).[12,13] With multiple and diverse targets, miRNAs control cellular processes such as proliferation,[14,15] division,[16] differentiation,[17] apoptosis,[18] protein secretion,[19] and viral infection.[20] The specific contribution of

The first two authors contributed equally to this work.

Correspondence: Burton B Yang, S110, Sunnybrook Research Institute, Sunnybrook Health Sciences Centre, 2075 Bayview Ave, Toronto M4N 3M5, Ontario, Canada. E-mail: byang@sri.utoronto.ca

selected miRNAs in hepatic disease development and progression has been described.[21] It has been suggested that miRNA may be related to hepatic steatosis formation in NAFLD through directly targeting downstream molecules. For example, miR-122, one of the most abundant microRNAs in the liver, regulates cholesterol biosynthesis in normal hepatocytes. miR-122 inhibition in normal mice resulted in reduced plasma cholesterol levels, increased hepatic fatty-acid oxidation, and a decrease in hepatic fatty-acid and cholesterol synthesis rates.[22] Another miRNA miR-17 appears to play roles in regulating liver functions.[23,24]

In this study, we tested the effects and relationship of DXM, miR-17-5p, and PPAR-α in the development of steatosis and fatty liver, using a miR-17-overexpressing transgenic mouse model. We found that DXM enhanced expression of PPAR-α and miR-17-5p. MiR-17-5p was found to repress PPAR-α expression, while PPAR-α could bind to the promoter of miR-17 and increase its transcription, forming a feedback loop in the regulation of steatosis and fatty liver development. We concluded that an inhibitor of miR-17-5p could be used to reduce the occurrence of steatosis and fatty liver development during Dexamethasone treatment. Finally, we found that drugs used for the treatment of metabolic disorders (WY-14643, Clofibrate, and Ciprofibrate), could decrease miR-17-5p expression levels and the DXM-induced steatosis and fatty liver development.

RESULTS

DXM induced expression of miR-17 and PPAR-α

DXM is a glucocorticoid class of steroid drugs with potent effects on anti-inflammation and immunosuppression and side-effects that include steatosis and fatty liver development.[4] Since PPAR-α regulates lipid metabolism,[6] we have, first of all, tested whether or not DXM affected PPAR-α expression. HepG2, SNU449, and mouse primary hepatocytes were treated with DXM, followed by real-time polymerase chain reaction (PCR) for quantitatively assessing PPARA mRNA levels and western blot analysis probed with an anti-PPAR-α antibody. DXM exhibited a dose-dependent effect of enhancing PPARA mRNA expression (**Figure 1a**). The effect of DXM on steatosis was confirmed in HepG2 cells by microscopic examination and steatosis quantification (**Supplementary Figure S1a**). Further analysis indicated that cells treated with DXM also expressed increased levels of miR-17-5p (**Figure 1b**). To analyze whether or not miR-17 plays a role in inducing steatosis, we examined HepG2 cells that had been stably transfected with the miR-17 expressing construct or a control GFP plasmid. Overexpression of miR-17 was confirmed by real-time PCR (**Supplementary Figure S1b**). The cells were treated with oleic acid followed by Oil Red O staining to reveal steatosis. Ectopic expression of miR-17 enhanced steatosis (**Figure 1c**; **Supplementary Figure S1c**).

We then validated the effects of miR-17 and DXM separately. HepG2 cells were transfected with miR-17-5p inhibitor or control oligonucleotides, followed by steatosis assay. The experiment showed that transfection with miR-17-5p inhibitor suppressed cell steatosis compared to the control (**Figure 1d**), confirming a role of miR-17-5p on inducing steatosis.

We examined the combined effect of DXM and miR-17-5p by treating HepG2 cells with miR-17-5p inhibitor and various concentrations of DXM, followed western blot analysis. While cells treated with DXM showed increase in PPAR-α expression, treatment with miR-17-5p inhibitor promoted PPAR-α levels (**Figure 1e**).

To examine the combined effects of DXM and miR-17-5p inhibitor, we treated HepG2 cells with DXM and with or without miR-17-5p inhibitor. Steatosis assay showed that DXM had a dose effect on promotion of steatosis and treatment with miR-17-5p inhibitor decreased the DXM-induced steatosis (**Figure 1f**).

miR-17 induced development of fatty liver in transgenic mice

We have previously developed a transgenic mouse line overexpressing miR-17.[25] After confirming increased expression of miR-17 (**Supplementary Figure S1d**), we examined whether or not the expression of miR-17 affected liver function in both transgenic (Tg) and wildtype (WT) mice and observed extensive steatotic change in the Tg liver but fewer in the WT liver (**Figure 2a**, with larger view provided, **Supplementary Figure S1e**). Oil Red O staining of the liver tissues further confirmed lipid accumulation in the Tg mice but not in the WT mice (**Figure 2b**). We examined a total of 42 miR-17 transgenic livers and 23 wildtype livers and grouped them to severe (at least seven large vacuoles per examination field as shown in **Figure 2a**, each around the size of a hepatocyte), medium (at least three vacuoles detected per examination field), and light (at least one vacuole per examination field) fatty liver. With this criterion, each photo was scanned with Image J software. Transgenic mice showed significant severer fatty liver incidences as compared with wildtype mice (**Figure 2c**, $P < 0.0001$).

Liver tissues from 10 randomly selected Tg mice and 10 WT mice were subject to analysis of triglyceride content. The Tg mice livers exhibited significantly higher levels of triglyceride than the WT mouse livers (**Figure 2d**, left). Measurement of cholesterol concentrations in total plasma indicated that the transgenic livers contained higher levels of cholesterol than the wildtype (**Figure 2d**, right).

PPAR-α is a direct target of miR-17-5p

Bioinformatic analysis indicated that miR-17 potentially targeted many mRNAs. We focused on those that are known to be important in lipid metabolism and in the development of fatty liver. After extensive analysis with western blotting using skin and livers from the miR-17 transgenic and wildtype mice and HepG2 cell lines stably transfected with miR-17 and the control vector, we found that PPAR-α was repressed (**Figure 3a**).

The 3'UTR of PPAR-α contains three potential target sites for miR-17-5p (**Figure 3b**). It has been reported that PPAR-α plays a crucial role in intracellular lipid metabolism.[26] It regulates the expression of proteins involved in the transport and β-oxidation of free fatty acids, predominantly in the liver.[27] PPAR-α knockout mice failed to show increased transcription of the enzymes involved in fatty acid transport and β-oxidation after stimulation with fibrates and developed intrahepatic accumulation of lipid droplets after 2 weeks of regular chow diet.[28] To validate targeting of PPAR-α by miR-17-5p, we generated three luciferase

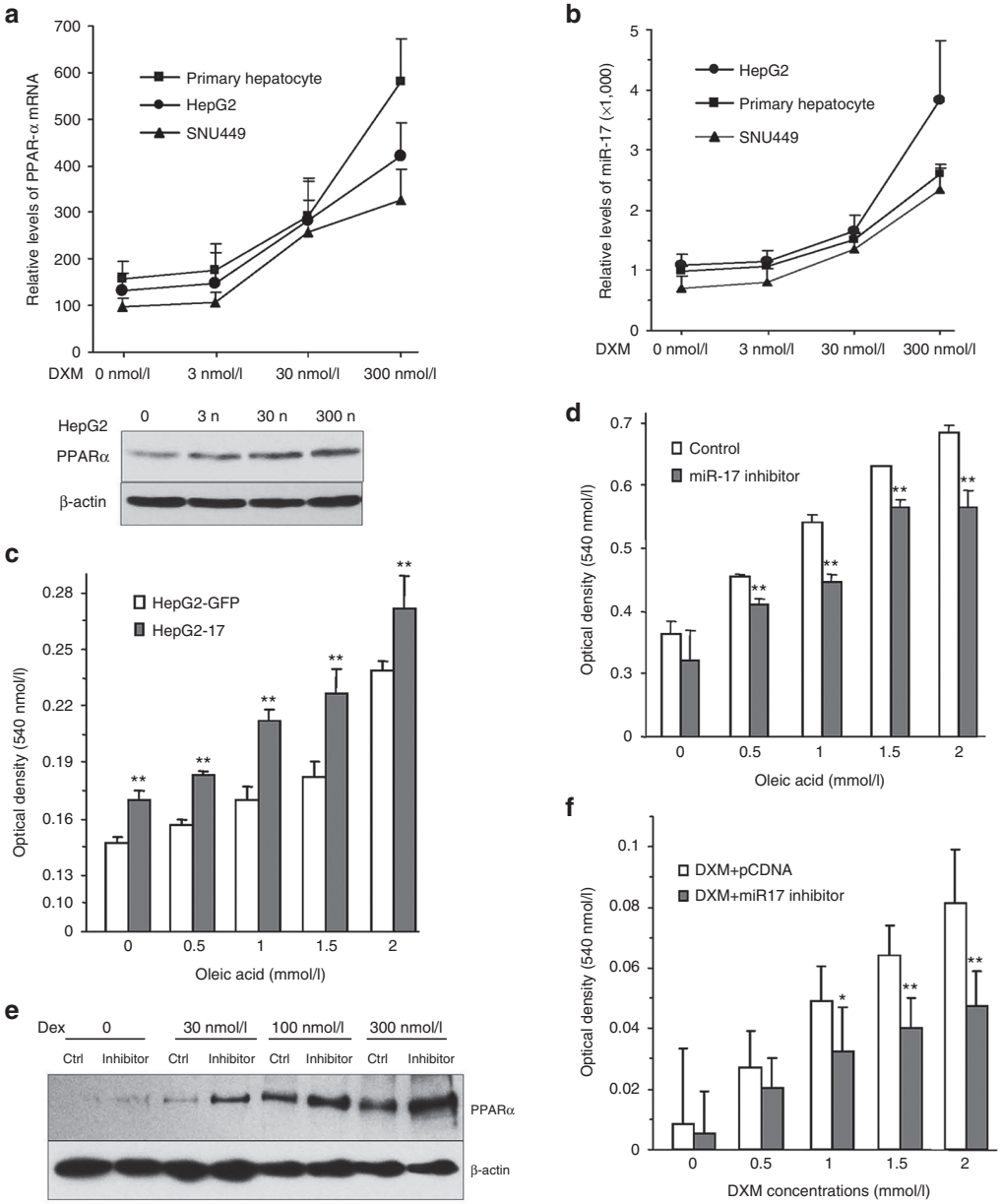

Figure 1 Dexamethasone induces expression of miR-17 and proliferator-activated receptor-α (PPAR-α). (**a**) Primary hepatocytes, HepG2, and SNU449 cells were treated with Dexamethasone at the indicated concentrations for 18 hours, followed by analysis of PPAR-α expression by real-time polymerase chain reaction using primers hu-ppara-SalI and hu-ppara-804R (upper) and western blotting (lower). Up to 300 nmol/l, Dexamethasone enhanced PPAR-α expression. (**b**) Analyzed for miR-17-5p levels showed that Dexamethasone treatment increased miR-17-5p expression. Error bars = SD, $n = 3$, $^*P < 0.05$, $^{**}P < 0.01$. (**c**) HepG2 cells stably transfected with miR-17 or GFP were subject to steatosis by treating the cells with different concentrations of oleic acid followed by Oil Red O staining. The stained color was extracted for optical density measurement. Expression of miR-17 promoted steatosis. $n = 3$, $^*P < 0.05$, $^{**}P < 0.01$. (**d**) HepG2 cells transfected with miR-17 inhibitor or the control oligos were treated with oleic acid at the concentrations indicated followed by steatosis assay. Introduction of miR-17 inhibitor decreased cell steatosis. Asterisks indicate significant differences. $^{**}P < 0.01$; ($n = 4$). (**e**) Protein lysates prepared from miR-17-5p inhibitor- and control oligos-transfected HepG2 cells, which were cultured in various concentrations of DXM, were subject to immunoblotting probed with antibodies against PPAR-α. The same membrane was reprobed for β-actin levels. Transfection with miR-17-5p inhibitor enhanced PPAR-α expression. (**f**) HepG2 cells were treated with dexamethasone with or without miR-17-5p inhibitor followed by steatosis assay. Treatment with miR-17-5p inhibitor significantly decreased steatosis.

constructs (Luc- PPAR-α1, Luc- PPAR-α2, and Luc- PPAR-α3, primer sequences provided in **Supplementary Figure S2a**) harboring the three fragments with the binding sites of miR-17 and three constructs in which the miR-17 target sites were mutated (Luc-PPAR-α mut1, Luc-PPAR-α2 mut2, and Luc-PPAR-α mut3) (**Figure 3b**, detail of the sequences are provided in **Supplementary Figure S2b**). HepG2 cells were cotransfected with miR-17 mimic and either one of the PPAR-α 3'UTR luciferase constructs or the mutant constructs, followed by luciferase activity analysis. Significant repression of luciferase activity was detected in the Luc-PPAR-α transfected cells (compared with luciferase empty vector or luciferase vector with no binding site sequence, G3R, $P < 0.01$), while transfection with the mutant constructs reversed the effect (**Figure 3c**).

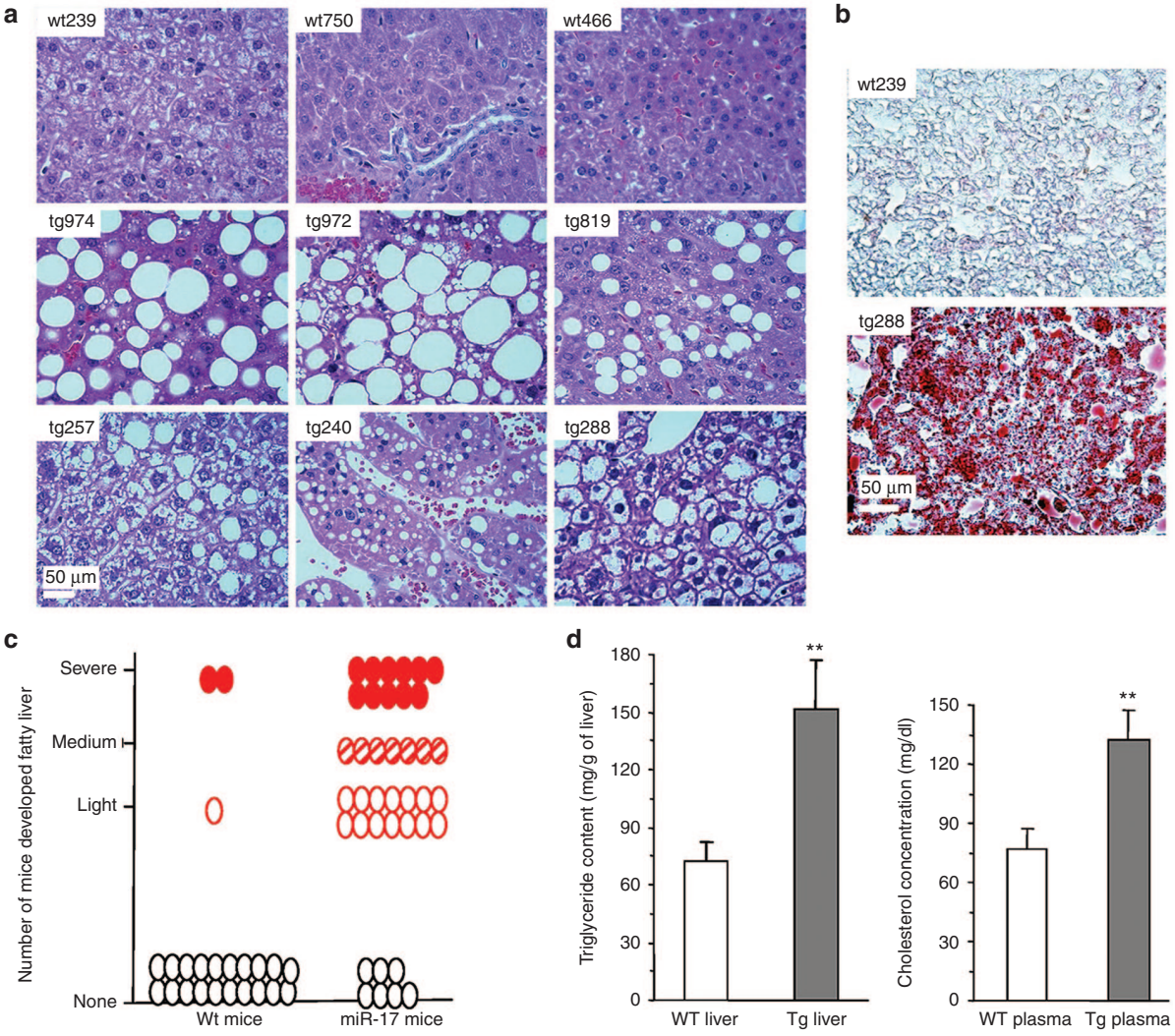

Figure 2 Expression of miR-17 promoted steatosis and fatty liver development. (**a**) Histological analysis of liver sections from miR17-transgenic (tg974, tg972, tg819, tg257, tg240, and tg288) and wild type (wt239, wt750, and wt466) mice showing copious fatty liver particularly in the transgenic livers. (**b**) Lipids in the liver sections were stained with Oil Red O. (**c**) Livers were harvested from transgenic and wild-type mice, sectioned, and subjected to H&E staining for examination of fatty liver. We grouped them to severe (at least seven large vacuoles, each around the size of a hepatocyte, occurring in nearby cells), medium (at least three vacuoles detected in nearby cells), and light (at least one vacuole detected) fatty liver. Transgenic mice tended to have fattier livers than wildtype mice (χ^2 test, $P < 0.0001$). (**d**) Left, Liver tissues were harvested from transgenic and wild type mice and evaluated for triglyceride content. Transgenic livers contained higher levels of triglyceride, $n = 10$; $^{**}P < 0.001$. Right, Total plasma levels were evaluated for cholesterol concentration. Transgenic livers contained higher levels of cholesterol, $n = 15$; $^{**}P < 0.001$.

To corroborate that PPAR-α could contribute to steatosis of HepG2 cell, we generated three small interfering RNAs (siRNA) constructs targeting PPAR-α. PPAR-α silencing was confirmed by western blot in the siRNA-transfected HepG2 cells (**Supplementary Figure S3a**). Transfection with PPAR-α siRNA promoted steatosis compared with those transfected with control oligonucleotides (**Figure 3d**, left), which was oleic acid concentration dependent (**Supplementary Figure S3b**).

To test whether or not PPAR-α was mediating the effect of miR-17 in inducing steatosis, we re-expressed PPAR-α in the miR-17-transfected cell line (**Supplementary Figure S3c**), followed by a steatosis assay. We detected significant decrease in steatosis occurrence in the miR-17 cells after retransfection with the PPAR-α expression construct compared with controls (**Figure 3d**, right), which was oleic acid concentration dependent (**Supplementary Figure S3d**). We also performed a comprehensive experiment to validate the effect of PPAR-α, miR-17-5p, and PPAR-α siRNA on steatosis. The experiment confirmed that miR-17-5p promoted steatosis, which was inhibited by PPAR-α (**Figure 3e**; **Supplementary Figure S4a**). Consistent with these results, treatment with PPAR-α inhibitor increased steatosis of HepG2 cells (**Figure 4a**). This confirmed that miR-17-enhanced HepG2 steatosis was mediated by PPAR-α pathway.

PPAR-α enhanced miR-17 expression

We then tested whether or not PPAR-α regulated miR-17 expression. HepG2 cells were transiently transfected with PPAR-α

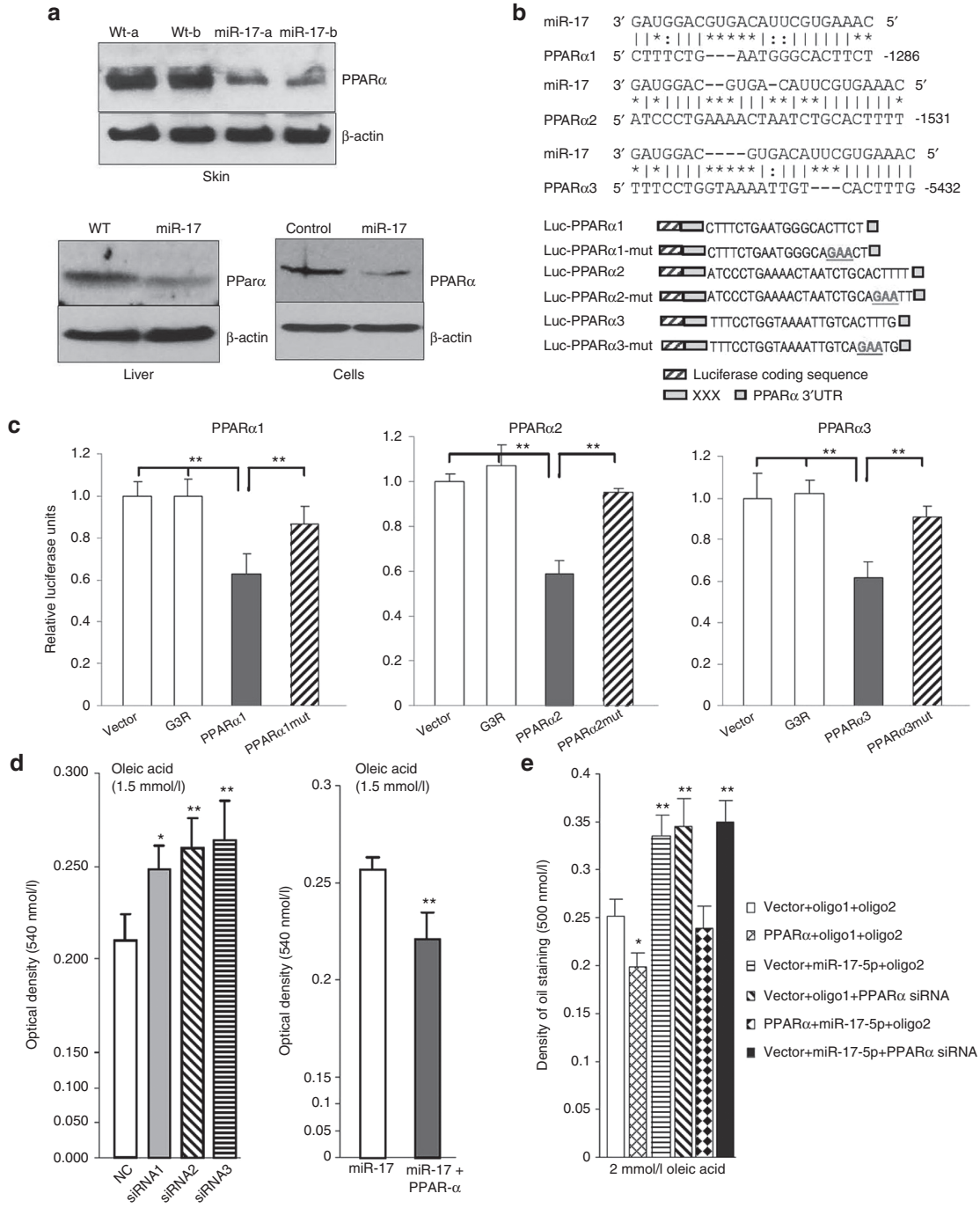

Figure 3 Targeting proliferator-activated receptor-α (PPAR-α) by miR-17. (**a**) Cell lysate prepared from miR-17 transgenic and wildtype liver and skin, and miR-17- and control vector-transfected HepG2 cells was analyzed on western blot for PPAR-α expression. PPAR-α was repressed by miR-17 expression. Staining for β-actin from the same membrane confirmed equal loading. (**b**) Upper, Computational analysis indicated that miR-17 potentially targeted PPAR-α located at nucleotides, 1,266–1,286, 1,506–1,531, 5,409–5,432. Lower, Three luciferase constructs were generated, each containing a fragment harboring the target site of miR-17, producing Luc-PParα1, Luc-PParα2, and Luc-PParα3. Mutations were also generated on the potential target sequence (red color), resulting in two mutant constructs Luc-Pparα1-mut, Luc-Pparα2-mut, and Luc-Pparα3-mut. (**c**) HepG2 cells were cotransfected with miR-17-5p mimic and a luciferase reporter construct, which was engineered with one of the three PPAR-α 3′UTR fragments, PPARα1 (left), PPARα2 (middle), and PPARα3 (right), harboring miR-17-5p target site or an appropriate mutants (PPARα1mut, PPARα2mut, and PPARα3mut). An unrelated sequence was used as a control (G3R) to compare with the vector, PPAR-α 3′UTR fragment, and PPAR-α1 mutant group. Unpaired Student's *t*-test for normal distribution was performed. The differences were considered statistically significant at $P < 0.05$. Asterisks indicate significant differences. *$P < 0.05$, $n = 6$. The luciferase activities decreased when the cells were transfected the PPAR-α luciferase constructs. Mutation of the binding site reversed miR-17-5p's effect. (**d**) Left, HepG2 cells transiently transfected with three PPAR-α siRNAs or the control oligo were subject to steatosis assay. Transfection with PPAR-α siRNAs enhanced steatosis. *$P < 0.05$, **$P < 0.01$, $n = 3$. Right, HepG2 cells stably transfected with miR-17 were transiently transfected with PPAR-α expression construct or a control vector. Transfection with PPAR-α reversed the effect of miR-17 resulting in decreased steatosis. **$P < 0.01$, $n = 3$. (**e**) HepG2 cells transiently transfected with PPAR-α, miR-17-5p mimic or/and Ppar-α siRNA, were subject to steatosis by treating the cells with 2 mmol/l oleic acid followed by Oil Red O staining. Expression of miR-17-5p or/and Ppar-α siRNA promoted steatosis, whereas expression of PPAR-α repressed steatosis. Asterisks indicate significant differences. *$P < 0.05$, **$P < 0.01$ ($n = 3$).

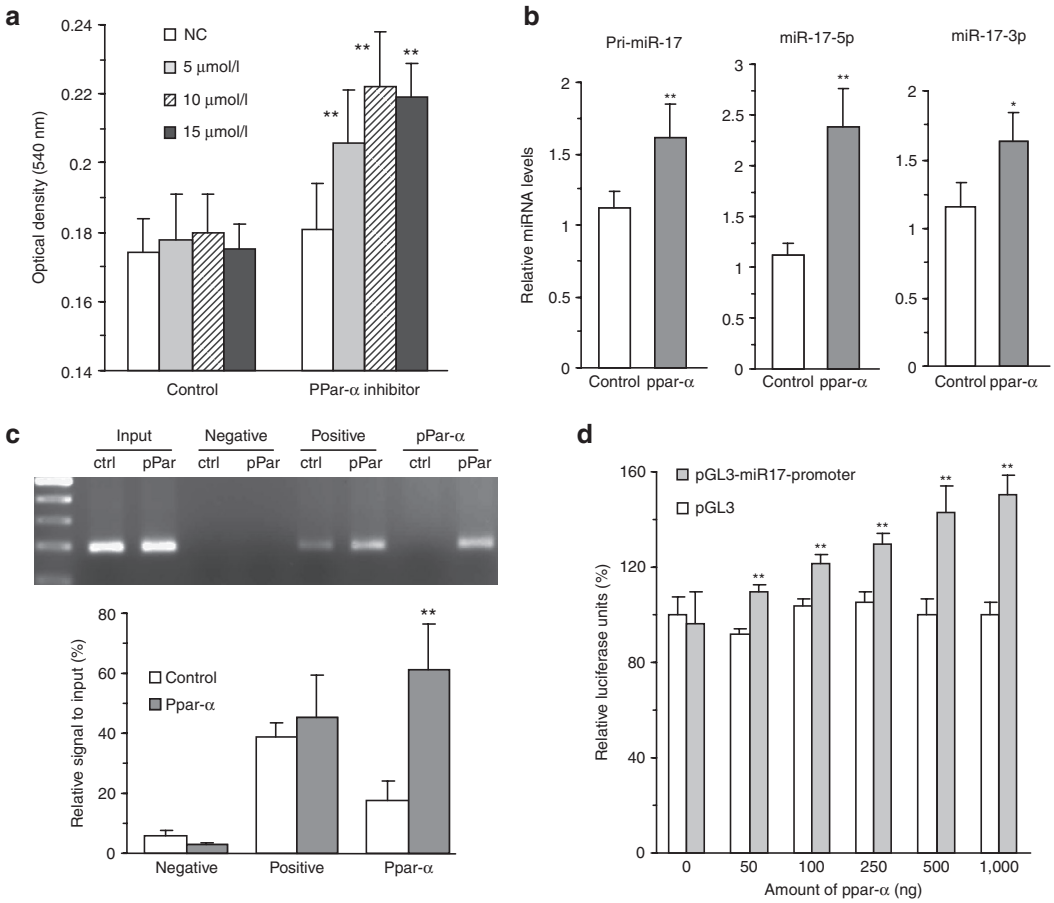

Figure 4 Expression of proliferator-activated receptor-α (PPAR-α) enhanced miR-17 transcription. (**a**) HepG2 cells were treated with PPAR-α inhibitor at the concentration indicated followed by steatosis assay. Treatment with PPAR-α antagonist (GW6471, Sigma) increased steatosis. Asterisks indicate significant differences. $^{**}P < 0.01$; $n = 4$. (**b**) Reverse transcription polymerase chain reaction showing PPAR-α transfected HepG2 cells expressed high levels of pri-miR-17 (left), miR-17-5p (middle), and miR-17-3p (right) compared to controls. Asterisks indicate significant differences. $^{*}P < 0.05$, $^{**}P < 0.01$; $n = 4$. (**c**) Upper, Chromatins of control- and PPAR-α-transfected HepG2 cells were isolated, digested, and immunoprecipitated with antibodies against PPAR-α, Histone H3 (positive control), and rabbit IgG (negative control), followed by PCR with specific primers (miR17-promot-for-PCR-F and miR17-promot-for-PCR-R) flanking a fragment of DNA in the miR-17 promoter. Lower, Graph showing that PPAR-α-transfected cells had more PPAR-α binding to miR-17 promoter. Asterisks indicate significant differences. $^{**}P < 0.01$; $n = 4$. (**d**) Luciferase assays were performed in HepG2 cells cotransfected with either PGL3 vector, or PGL3-miR-17-promoter, and various dose of PPAR-α. Increased PPAR-α doses enhanced luciferase activities. Asterisks indicate significant differences. $^{**}P < 0.01$; $n = 4$.

expression construct, followed by analysis of miR-17 expression. We found that the transfected cells expressed significantly higher levels of Pri-miR-17, miR-17-5p, and miR-17-3p as compared with the vector control (**Figure 4b**). It appeared that PPAR-α regulated miR-17 transcription. Chromatin from PPAR-α- and control-transfected HepG2 cells were isolated, digested, and immunoprecipitated with antibodies against PPAR-α, Histone H3 (serving as a positive control), and rabbit IgG (serving as a negative control), followed by PCR with specific primers flanking a fragment of DNA in the miR-17 promoter. It showed that antibody against PPAR-α, which precipitated PPAR-α (**Supplementary Figure S4b**), pulled down miR-17 promoter (**Figure 4c**).

A luciferase construct was generated by inserting the miR-17 promoter into the pGL3-Basic Vector (Promega) as indicated (**Supplementary Figure S4c**), followed by transfection of HepG2 cells with this miR-17 promoter-containing pGL3 construct or the control pGL3 plasmid at various amounts. Insertion of miR-17 promoter increased luciferase activities significantly compared with the control (**Figure 4d**).

miR-17 expression promoted DXM-induced fatty liver development

To test whether miR-17-5p could modulate DXM-induced fatty liver development, we injected the miR-17 transgenic mice with DXM at a concentration of 50 mg/kg everyday for 3 days. The mice were kept for an additional 3 days. At this concentration, DXM treatment enlarged the miR-17 livers significantly, but did not show a significant effect on the wildtype group (**Figure 5a**, upper). Also, the miR-17 livers were yellow in color, indicating the presence of fatty liver (**Figure 5a**, lower). However, the miR-17 mouse livers showed decreased weight compared with wildtype group without DXM treatment, although not reaching a significant level. The most likely reasons were that the mice used in this experiment were young (3–4 weeks old), the livers of these young miR-17 mice had not developed fatty liver significantly, and expression of miR-17 retarded some organs, such as liver growth during development.[25]

Histological analysis also exhibited large number of lipid vacuoles in the miR-17 liver treated with DXM, another indication of fatty livers (**Figure 5b**). The paraffin sections were subject

to immunohistochemical staining. A clear downregulation of PPAR-α was confirmed in the miR-17 transgenic mice compared with the wildtype (**Figure 5c**). The frozen sections of livers were subject to Oil Red O staining. The miR-17 livers showed many more pink droplets than the wildtype livers (**Figure 5d**, upper). Quantification of the pink droplets indicated significant increase in DXM-treated livers (**Figure 5d**, lower). In this experiment, application of DXM induced fatty liver in both miR-17 transgenic and

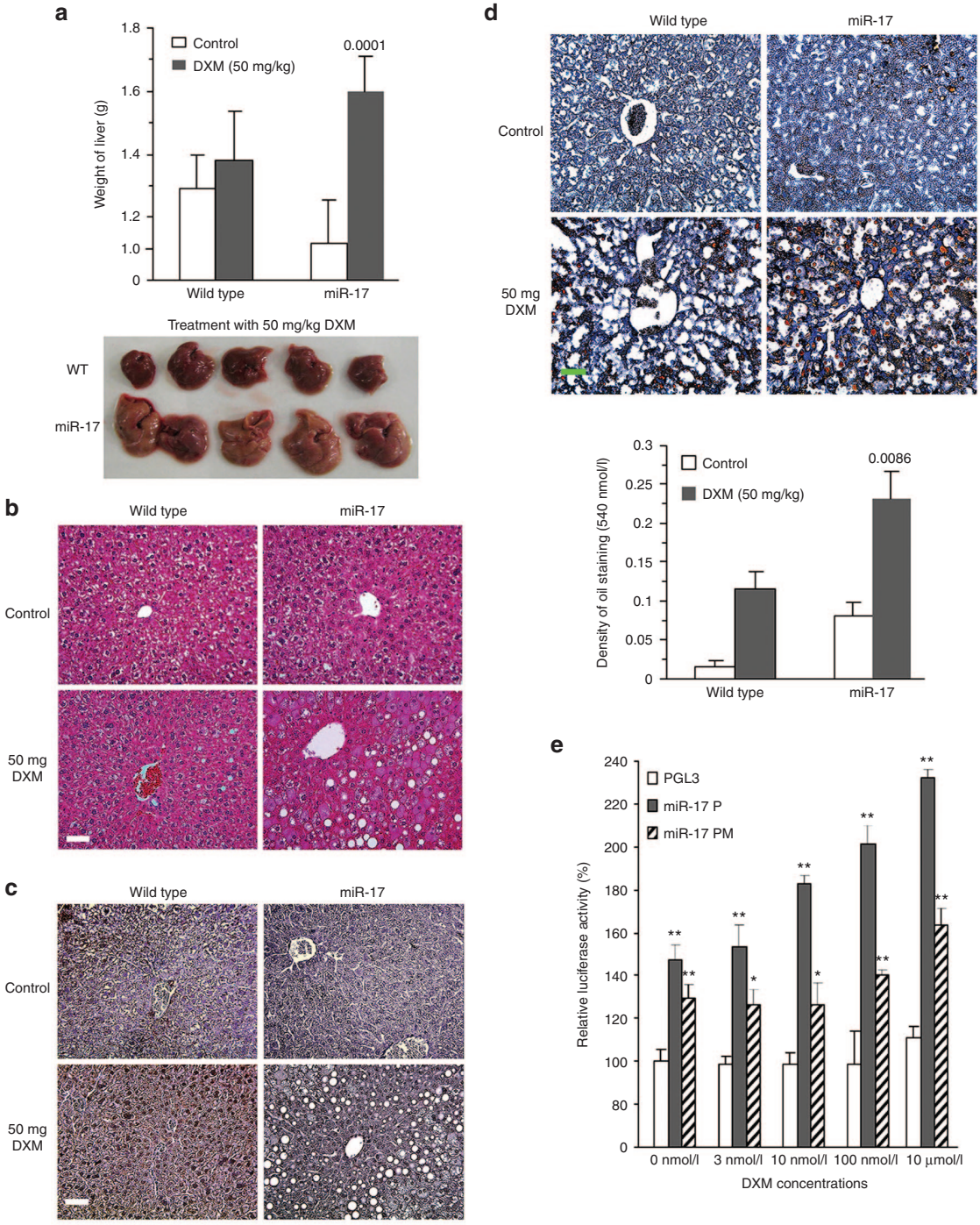

Figure 5 Development of fatty liver in miR-17 transgenic mice induced by dexamethasone (DXM). (**a**) Upper, Although the weight of liver decreased in the miR-17-transgenic mice, treatment with DXM (50 mg/kg DXM) significantly increased their liver weight compared with wildtype. Asterisks indicate significant differences, $n = 15$. Lower, Typical photo of livers from miR-17-transgenic and wild-type mice. (**b**) In HE staining, the miR-17 transgenic mice exhibited large number of lipid vacuoles in the miR-17 liver treated with DXM. (**c**) Immunohistochemistry showing that the miR-17 transgenic mice expressed low levels of proliferator-activated receptor-α (PPAR-α) in miR-17 liver treated with DXM. (**d**) Upper, in Oil Red O staining assay, miR-17 transgenic livers displayed more oil droplet stained by Oil Red O in the miR-17 liver treated with DXM. Lower, Quantification analysis indicated that DXM had significant effect on steatosis, $n = 12$. Scale bars for **b–d**, 50 μm. (**e**) Luciferase assays were performed in HepG2 cells transfected with PGL3 vector, PGL3-miR-17-promoter (miR-17-P), or PGL3-miR-17-promoter-mutant (miR-17-PM) in the presence of DXM at various concentrations. DXM enhanced luciferase activities. Asterisks indicate significant differences. $^*P < 0.05$, $^{**}P < 0.01$; $n = 4$.

wildtype mice. However, the miR-17 transgenic group developed serious fatty liver. To test if DXM could enhance miR-17-5p activity through miR-17 upregulation, we conducted a luciferase assay, by transfecting HepG2 cells with the luciferase plasmid pGL3, containing the miR-17 promoter or the mutant promoter, in which two PPAR-α binding sites were mutated (**Supplementary Figure S4c**). Luciferase assay showed that DXM enhanced luciferase activity when the construct was inserted with the miR-17 promoter (**Figure 5e**). Mutation of the PPAR-α binding sites significantly decreased luciferase activity, but could not fully suppress the luciferase activity. Perhaps, PPAR-α could bind to other areas of the promoter fragment resulting in decreased luciferase activities.

Inhibition of miR-17-5p function abolished DXM-induced fatty liver development

To test the possibility of using miR-17-5p inhibitor as an agent to alleviate DXM-induced fatty liver development, we treated mice with different concentrations of DXM and found that DXM at a concentration of 100 mg/kg could induce formation of fatty livers effectively. The miR-17 transgenic and wildtype mice were treated with DXM (100 mg/kg) combined with miR-17-5p inhibitor. The experiment showed that inclusion of miR-17-5p inhibitor decreased the liver weight of both types of mice (**Figure 6a**, upper). In the miR-17 transgenic mice, treatment with DXM showed yellow livers, but addition of miR-17-5p inhibitor abolished this effect (**Figure 6a**, lower). We then examined the effect of miR-17-5p inhibitor on PPAR-α expression by western blotting. Protein lysates were prepared from liver tissues and subject to immunoblotting probed with antibodies against PPAR-α. We confirmed that both miR-17 transgenic and wildtype mice expressed high levels of PPAR-α after treatment with DXM and miR-17-5p inhibitor (**Figure 6b**).

Histological analysis of the livers indicated that vacuoles in both miR-17 transgenic and wildtype livers significantly decreased when the mice were treated with miR-17-5p inhibitor (**Figure 6c**). The liver sections were subject to Oil Red O staining. Treatment with miR-17-5p inhibitor decreased Oil Red O staining in both the wildtype and miR-17 transgenic mice significantly (**Figure 6d**). Immunohistochemical staining showed that PPAR-α levels were lower in the miR-17 liver than in the wildtype liver but higher in the liver treated with miR-17-5p inhibitor (**Supplementary Figure S5a**).

The side-effect of DXM-induced steatosis could be inhibited by chemicals that decreased miR-17-5p levels

Our results showed that PPAR-α and miR-17-5p are two essential factors that affected steatosis and fatty liver development. We sought to find chemical drugs that modulate expression of PPAR-α and miR-17-5p and inhibit DXM-induced steatosis. We selected Bezafibrate, Fenofibrate, Gemfibrozil, Clofibrate, Ciprofibrate, and WY-14643 in the *in vitro* study. All of these chemicals are potent PPAR-α agonists. While the first five reagents are widely used in clinic, the last one is still in preclinical trial. HepG2 cells were treated with these chemicals, and subject to real-time PCR analysis for expression of PPAR-α and miR-17-5p. We found that treatment with all chemicals/drugs promoted PPAR-α expression (**Figure 7a**). However, only Clofibrate, Ciprofibrate, and WY-14643 could decrease miR-17-5p levels (**Figure 7b**). This effect was more potent when combined with DXM. Western blot analysis produced consistent results when the cells were treated with WY-14643, Clofibrate, and Ciprofibrate (**Supplementary Figure S5b**). The treatments produced inconsistency in protein and mRNA levels could be resulted from post-transcriptional regulation. Interestingly, only the three chemicals/drugs that decreased miR-17-5p levels and enhanced PPAR-α expression could decrease steatosis in the cells treated with DXM (**Figure 7c**). These results provide evidence indicating the essential roles of miR-17-5p in modulating DXM-induced steatosis, and highlight the importance of selection of suitable PPAR-α activating reagents to prevent steatosis in DXM treatment. Those chemicals with both PPAR-α activation and miR-17-5p repression might be the proper choice in clinic. The effects of these factors on steatosis and fatty liver development, as well as their relationship, are provided in **Figure 7d**. Application of DXM enhanced expression of both miR-17 and PPAR-α of liver cells, which played different roles in the progression of steatosis and fatty liver development. Current study indicated that expression of miR-17-5p promoted steatosis progression and fatty liver development, whereas activation of PPAR-α repressed these processes. Final physiological outcome relies on the interaction between miR-17-5p and PPAR-α. Since miR-17-5p targeted PPAR-α and repressed its expression, while PPAR-α promoted miR-17 transcription, any reagents modulating the expression of one molecule would affect the other, and might change the liver cell phenotype. In our study, we applied miR-17-5p inhibitor and PPAR-α agonists to interrupt this feedback regulation loop, and found that repression miR-17-5p expression or application of PPAR-α activators was a potentially valuable strategy to reverse DXM-induced steatosis and fatty liver development.

DISCUSSION

Steatosis is the earliest stage of NAFLD and is frequently observed in metabolic dysfunctions that preceed human hepatocellular carcinoma. Hepatic steatosis is often self-limited, but it can also progress to NASH.[29,30] Since cell injury may occur, when the capacity of hepatocytes to safely store fat is overwhelmed by continued uptake, local synthesis, or impaired egress of fatty acids, these fatty acids then become toxic to the cell, causing cell death by the direct effects of lipid mediators on apoptosis.[31] Alternatively, liberation of oxidized lipids and their peroxidation products (chemotactic aldehydes and organic acids) may be instrumental in recruiting and perpetuating the inflammatory response that characterizes NASH.[29] Steatosis could therefore provide the foundation for fatty liver and NASH, which can lead to hepatic fibrosis or cirrhosis, and may progress to hepatocellular carcinoma.[32] We found that ectopic expression of miR-17-5p could induce steatosis and fatty liver development by repressing PPAR-α expression.

In our study, ectopic expression of mature miRNA-17-5p significantly reduced expression of PPAR-α through targeting PPAR-α 3'UTR (**Figure 3**). It is anticipated that disruption of PPAR-α signaling can promote lipid uptake and/or inhibit lipolysis as evidenced by increased lipid accumulation. Since PPAR-α belongs to the nuclear hormone receptor superfamily, it has the potential to regulate gene transcription (including miRNAs).

In our study, we uncover the relationships of miR-17-5p, DXM, and PPAR-α in cell steatosis and development of fatty liver.

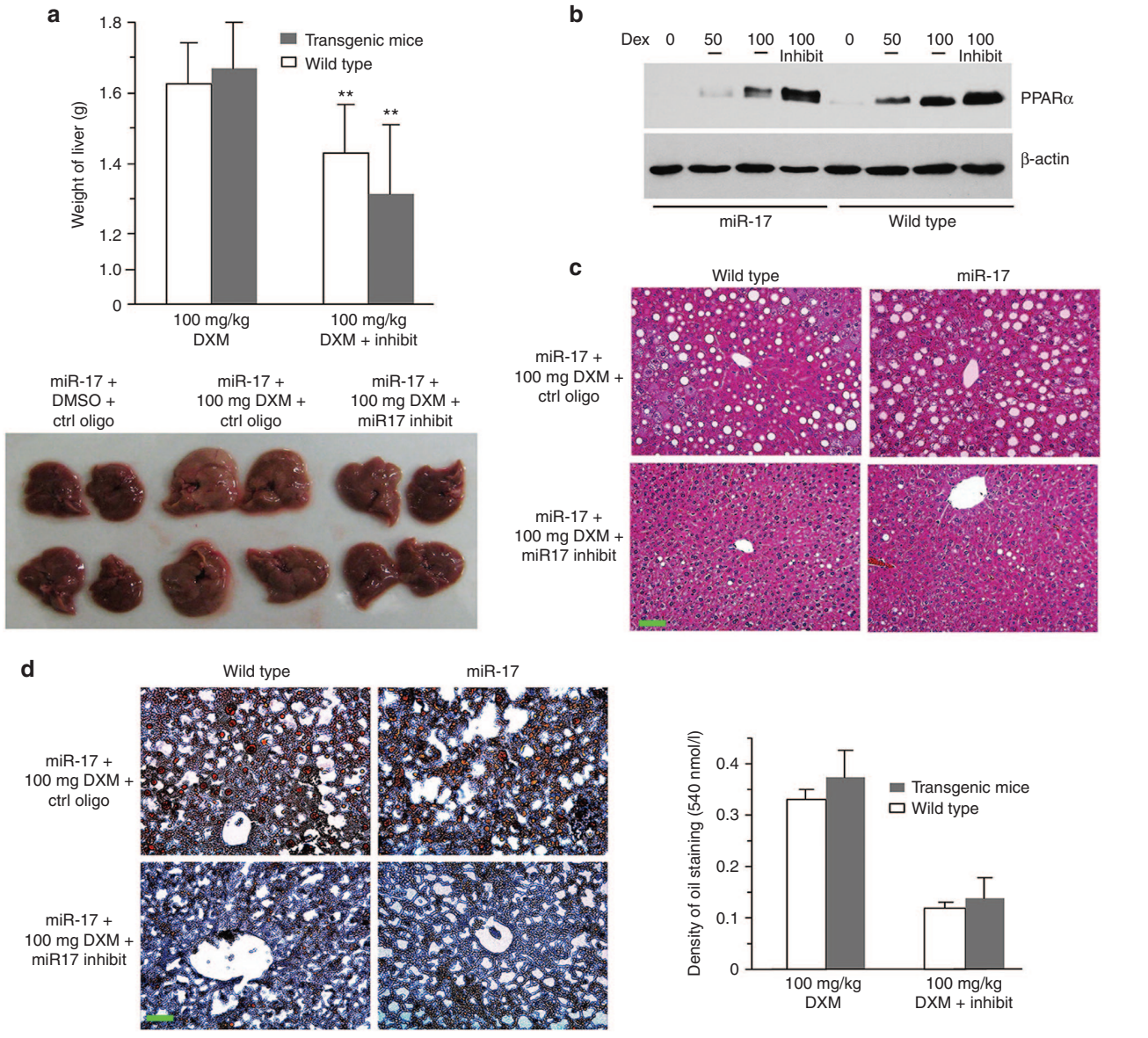

Figure 6 miR-17-5p inhibitor enhanced proliferator-activated receptor-α (PPAR-α) expression and alleviated dexamethasone (DXM)-induced fatty liver. (**a**) Upper, Treated with higher concentration of DXM (100 mg/kg), the miR-17-transgenic and wild-type mice had similar liver weight. However, treatment with control oligo (ctrl oligo) with random sequence or miR-17-5p inhibitor decreased liver weight of both the wildtype and miR-17-transgenic mice. Asterisks indicate significant differences. $^{**}P < 0.01$; $n = 15$. Lower, Typical photo of miR-17 transgenic livers treated with or without DXM and miR17-5p inhibitor. (**b**) Protein lysates prepared from liver tissues treated with different concentration of DXM and miR-17-5p inhibitor were subject to immunoblotting probed with antibodies to PPAR-α and β-actin. Immunoblot showed that Both miR-17 transgenic and wildtype mice expressed high levels of PPAR-α after treatment with DXM and miR-17-5p inhibitor. (**c**) The miR-17 transgenic and wildtype livers treated with or without DXM and miR-17-5p inhibitor were subject to HE staining. Vacuoles in both miR-17 transgenic and wildtype livers significantly decreased when the mice were treated with miR-17-5p inhibitor. (**d**) Left, The liver sections were also subject to Oil Red O staining. Treatment with miR-17-5p inhibitor decreased Oil Red O staining. Right, Quantification analysis indicated that treating the mice with miR-17-5p inhibitor significantly decreased oil accumulation in the livers. Asterisks indicate significant differences. $^{**}P < 0.01$; $n = 12$. Scale bars for **c**,**d**, 50 μm.

In the first part of our work (Figures 1–4), while we provided evidence to understand the relationship, we found a feed-back loop regulation between miR-17-5p and PPAR-α. Computational analysis showed that PPAR-α is a potential target of miR-17-5p: there are three potential binding sites in PPAR-α 3'UTR for miR-17-5p (Figure 3). Ectopic expression of miR-17 repressed PPAR-α protein levels in the miR-17-transfected cells, and in the skin and liver of miR-17 transgenic mice. Luciferase assay further confirmed that miR-17-5p could repress luciferase activities when the constructs harbored one of the three binding sites. On the other hand, PPAR-α could directly bind to the promoter of the miR-17–92 cluster (Figure 4). In the luciferase assay, we showed that this binding significantly enhanced promoter activities. This feed-back loop regulation suggests that, while both miR-17-5p and PPAR-α played important roles in the progression of steatosis and fatty liver development, the feed-back loop may facilitate a balance for the regulation. Indeed, DXM could upregulate PPAR-α expression, but the overall outcome of DXM is to prevent

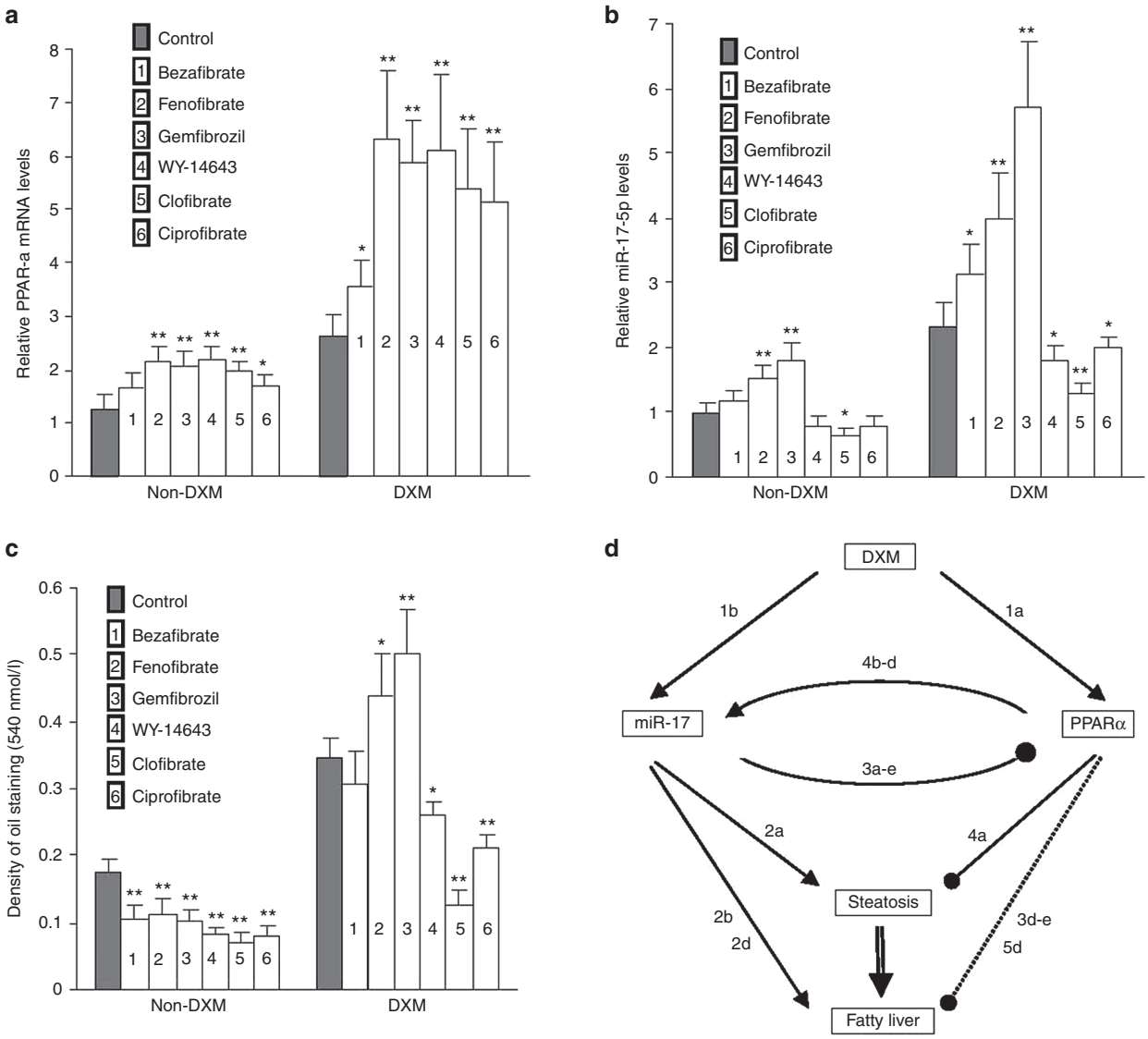

Figure 7 Selecting chemicals that can decrease the side-effect of dexamethasone (DXM) in inducing steatosis. (**a**) Bezafibrate, Fenofibrate, Gemfibrozil, Clofibrate, Ciprofibrate, and WY-14643 were all dissolved in Dimethyl sulfoxide (*DMSO*). Total RNAs were prepared from HepG2 cells treated with 500 μmol/l Bezafibrate, Fenofibrate, Gemfibrozil, Clofibrate, Ciprofibrate, or 100 μmol/l WY-14643 for 48 hours, followed by real-time polymerase chain reaction analysis. Cells treated with all drugs/chemicals produced significantly higher levels of proliferator-activated receptor-α (PPAR-α) transcription after cultured with or without DXM. (**b**) The RNAs were also subject to assay for miR-17-5p levels. Without DXM treatment, Fenofibrate and Gemfibrozil increased, while Clofibrate decreased miR-17-5p levels. In the presence of DXM, Bezafibrate, Fenofibrate, and Gemfibrozil increased, while WY-14643, Clofibrate, and Ciprofibrate decreased miR-17-5p levels. (**c**) In cell steatosis assay by treating the cells with 0.25 mmol/l Oleic acid for 24 hours, all chemicals decreased steatosis without the treatment of DXM. However, in the presence of DXM, Fenofibrate, and Gemfibrozil increased, while WY-14643, Clofibrate, and Ciprofibrate decreased steatosis. (**d**) Diagram showing the effects of glucocorticoid, miR-17, and PPAR-α on steatosis and development of fatty liver. Results from the figures are indicated by figure numbers.

inhibition of steatosis and fatty liver development, rather than directly inducing these processes.

PPAR-α appears to be a dual-role regulator in the formation of steatosis and fatty liver. Inhibition of PPAR-α activity promoted steatosis. In addition, the levels of PPAR-α were much lower in the fatty livers than in the normal livers. Although these are correlational results, they support the notion that PPAR-α can inhibit fatty liver development. PPAR-α could bind to miR-17 promoter and promote miR-17-5p expression. This seemed to produce an opposite function in the development of steatosis and fatty liver. However, the upregulated miR-17-5p could turn back to inhibit PPAR-α expression, forming the feed-back loop. This feed-back loop would allow the system to achieve a balance when treated with DXM or other agents involved in the system.

Nevertheless, repression of PPAR-α levels appears to be an essential step in the induction of steatosis and fatty liver development regulated by miR-17-5p. It should be noted that there are many potential targets of miR-17-5p. Other targets (for example, ATP-binding cassette transporter ABCA1) could also contribute to the miR-17-5p-induced steatosis and fatty liver development. Further studies are needed to provide a comprehensive picture for understanding miR-17-5p induction of steatosis and fatty liver development.

Our experiments show that miR-17-5p is a key player in mediating DXM's effect on inducing steatosis and fatty liver formation

(**Figure 7**). Even without DXM treatment, upregulation of miR-17-5p could induce steatosis in cells and fatty liver formation in mice. High levels of miR-17-5p expression (in the miR-17-transgenic mice) increased the sensitivity of mice to DXM-induced fatty liver development compared to wildtype mice, which showed little change when treated with a low concentration of DXM. Thus, we sought to develop an approach to inhibit steatosis and fatty liver formation in the second part of our studies. We found that the inhibitor of miR-17-5p could sufficiently inhibit steatosis and fatty liver development. While high concentration of DXM could induce development of fatty liver, injection of miR-17-5p inhibitor could completely inhibit fatty liver development. These results suggest that miR-17-5p inhibitor can desensitize livers to DXM treatment. It may thus be a supplementary agent for those who are being treated with DXM and could potentially develop fatty liver as a result of the side-effect of DXM.

We also screened a number of chemicals/drugs that are known to play roles in treating hypercholesterolemia. It was expected that many of these chemicals/drugs might increase PPAR-α expression. However, we looked for chemicals/drugs that could decrease miR-17-5p levels. Clofibrate, and Ciprofibrate, and WY-14643 could all decrease miR-17-5p expression and inhibit steatosis when being combined with DXM. In particular, Clofibrate showed the strongest effect on reducing miR-17-5p expression of steatosis levels. Clofibrate, an organic compound, is a lipid-lowering agent and is used for controlling high cholesterol in the blood. However, this drug was discontinued in 2002 due to adverse affects. Ciprofibrate is a fibrate, and WY-14643 is a PPAR-α agonist, both of which are used for metabolic disorders. Since both Ciprofibrate and WY-14643 could promote PPAR-α expression and inhibit the process of steatosis, they are the ideal agents to be combined with DXM in the treatment of anti-inflammation and immunosuppression, as well as in some cases for cancer patients. We anticipate these findings will stimulate further research into chemical agents that reduce DXM and glucocorticoid-induced side effects.

MATERIALS AND METHODS

Generation of constructs and genotyping of miR-17 transgenic mice. A cDNA sequence containing two human pre-miR-17 units was inserted into a mammalian expression vector pEGFP-N1 in the restriction enzyme sites BglII and HindIII. Transgenic mice expressing miR-17 were generated as described previously.[25]

A luciferase reporter vector (pMir-Report; Ambion) was used to generate the luciferase constructs. Three fragments of the 3'UTR of mouse PPAR-α were cloned by RT-PCR using three pairs of primers (mus-ppara-mir17a-SacI and mus-ppara-mir17a-MluI for fragment-1; mus-ppara-mir17a-SacI and mus-ppara-mir17b-MluI for fragment-2; mus-ppara-mir17c-SacI and mus-ppara-mir17c-MluI for fragment-3). Three mutation primers (mus-ppara-mir17a-MluI-mut, mus-ppara-mir17b-MluI-mut, and mus-ppara-mir17c-MluI-mut) were used to generate mutations in the miR-17-5p target sites. PCR products were digested with SacI and MluI and the fragments were inserted into a SacI- and MluI opened pMir-Report luciferase vector.

The promoter of miR-17 was cloned using two primers miR17promotSacI and miR17promotHindIII. The first potential PPAR-a binding site was mutated with two primers Dex-prom-mut1-BglII-F and Dex-prom-mut1-BglII-R, while the second potential binding site was mutated with two primers Dec-prom-mut2-XhoI-R and Dec-promoter-XhoI-F.

Real-time PCR. The experiment was performed as previously described.[33,34] In brief, total RNA was extracted from ~1×10^6 cells or ~50 mg tissues, and subject to cDNA synthesis using 1 μg RNA. Successive PCR was performed by QuantiMir-RT Kit using 1 μl cDNA as a template (Qiagen, Valencia, CA, miScript Reverse Transcription Kit, cat#218060; miScript Primer Assay, cat#218411; miScriptSYBR GreenPCR Kit, cat#218073).

Western blot. Cell lysates were obtained from the cultures or extracted from frozen tissues and subjected to SDS-PAGE electrophoresis and western blot analysis as described.[35,36]

Oil Red O staining. Frozen liver sections were fixed in 10% formalin and briefly washed with water for 10 minutes. The sections were rinsed with 60% isopropanol and stained with freshly prepared Oil Red O working solution for 15 minutes. Sections were rinsed with 60% isopropanol, lightly stained with aluminium hematoxylin and mounted in glycerine jelly.

Induction of steatosis in HepG2 cell by oleic acid treatment. HepG2 cells were cultured in 96-well tissue culture plates to sub-confluence. The medium was changed into serum-free Dulbecco's modified Eagle's medium, followed by treating the cells with 200 μl oleic acid (OA) solution containing different concentrations (0.25–2 mmol/l) of OA overnight. The medium was removed and the cells were treated with 100 μl fixative solution (10% formalin) at room temperature for 10 minutes, followed by microscopic examination.

For quantification, steatosis was induced by OA and stained with Oil Red O. After washing and completely drying, 100 μl of 100% isopropanol was added to each well, followed by incubating at room temperature for 10 minutes to release Oil Red O from steatosis staining. The extraction solution was transferred to another 96-well plate which was subjected to OD measurement at a wavelength of 540 nm using a microplate reader (Bio-Tek Instrument, Winooski, VT).

Liver triglyceride content measurement. Liver samples were weighted (100–300 mg) and 300 μl of ethanolic KOH (2 parts EtOH mixed with 1 part 30% KOH) were added to each sample, followed by incubation at 55 °C overnight. Diluted EtOH (H_2O:EtOH=1:1) was added into each tube to bring the volume to 1 ml. The tubes were centrifuged for 5 minutes and the supernatant was transferred into new tubes. The diluted EtOH was added again into each tube to bring the volume to 1.2 ml. After vortex, 200 μl of the mixture was transferred into new Eppendorf tubes in triplicates, followed by addition of 215 μl 1M $MgCl_2$ and incubation on ice for 10 minutes. The tubes were centrifuged for 5 minutes and the supernatant was transferred into new tubes.

Triglyceride reagent (Sigma, St. Louis, MO, catalog # F6428) was reconstituted according to manufacturer's instructions for determination of glycerol content. One milliliter of reconstituted reagent was pipetted into each cuvette. Liver lysates, standards, and control blanks were added into separate cuvettes, and incubated at 37 °C for 15 minutes. Absorbance values were measured at 540 nm.

Luciferase assay. The assay was performed as previously described.[35]

Chromotin immunoprecipitation (ChIP) assay. ChIP was performed using Simple ChIP chromatin IP kit (Cell Signaling) according to the manufacturer's instructions. Briefly, cells were treated with formaldehyde solution. The chromatin was isolated, digested, and immunoprecipitated with antibody against PPAR-α. The captured chromatin was eluted, uncross-linked, and the DNA was recovered. The ChIP isolated DNA was subject to PCR using specific primers (miR17-promot-for-PCR-F and miR17-promot-for-PCR-R) flanking a piece of DNA fragment of the miR-17 promoter region.

DXM induction of mouse fatty liver. The miR-17 transgenic mice used in this experiment were between 4–5 weeks of age. They were maintained under 12-hour light/12-hour dark photoperiod at room temperature of 22–23 °C and relative humidity of 50%. All animal experiments

were approved by the Animal Care Committee of Sunnybrook Research Institute, Ontario, Canada.

DXM sodium phosphate (Omega, Montreal, Canada) diluted in 0.9% NaCl was administered i.p. to wildtype or miR-17 transgenic mice at a dose of 50 mg/kg or 100 mg/kg body weight every day for 3 days. Each group had 15 mice. The mice were sacrificed on day 6. In the group treated with miR-17-5p inhibitor (GenePharma, Shanghai), miR-17-5p inhibitor (miR-17-5p antisense mimic, 6 μg) was injected i.p. with the inhibitor-PEG-Au NP complexes 12 hours before DXM injection, and repeated 48 hours after initial injection.

Synthesis of the deliver complexes (inhibitor-PEG-Au NP) was performed as previously described.[37] Briefly, 20 nmol thiol modified miR-17-5p inhibitor was dissolved in 800 μl of RNase-free water. The mPEG-SH (PG1-TH-2k, Nanocs) was mixed with miR-17-5p inhibitor (1:20 molar ratio). Then 10-nm gold nanoparticles (AuNP, Cytodiagnostics) were mixed with miR-17-5p inhibitor-PEG at a weight ratio of 1:20 for conjugation. The mixture was gently shaken at 60 °C for 30 minutes and transferred into a syringe.

Mice were sacrificed on day 6 for liver harvest. The left lobe of the liver was kept frozen for immunoblotting or PCR, while additional parts were fixed in 10% formalin. After 24 hours, the right lobe of liver was processed to obtain frozen sections, followed by Oil Red O staining and counterstaining with Mayer's Hematoxylin. To quantify Oil Red O staining, 200 μl of isopropanol was added to the sections and incubated for 10 minutes with gently shaking. The supernatant was transferred to 96-well plates. Absorbance value was measured at 540 nm with isopropanol as blank. A fragment of liver was processed to paraffin embed and sectioning. The sections were subjected to either H&E staining or immunohistochemical staining with antibodies against PPAR-α (Santa Cruz, Dallas, TX, Cat# sc-9000).

Statistical analysis. All experiments were performed in triplicate or higher. Data were expressed as mean ± SE. Unpaired Student's *t*-test and χ^2 test for normal distribution was performed. The differences were considered statistically significant at $p < 0.05$.

SUPPLEMENTARY MATERIAL

Figure S1. Expression of miR-17.
Figure S2. Sequences of primers and fragments of PPAR-α 3'UTR.
Figure S3. Effects of silencing and overexpression of PPAR-α.
Figure S4. Targeting analysis of PPAR-α by miR-17-5p.
Figure S5. Effects of PPAR-α inhibitors.

ACKNOWLEDGMENTS

This work was supported by China-Canada Joint Health Research Grant (from the National Natural Science Foundation of China, No. 30911120492, to Y.Z. and Canadian Institutes of Health Research, CCI 201205, B.B.Y.), a grant from Canadian Institutes of Health Research (CHRP 462341-2014) and Natural Sciences and Engineering Research Council of Canada (CPG 134747) to S.N.K and B.B.Y, and a Discovery Grant from the Natural Sciences and Engineering Research Council of Canada (NSERC; 227937-2012) to B.B.Y., who is the recipient of a Career Investigator Award (CI 7418) from the Heart and Stroke Foundation of Ontario. W.W.D. is supported by a fellowship from Canadian Breast Cancer Foundation of Ontario. F.L. is supported by a Scholarship from China Scholarship Council.

REFERENCES

1. Anstee, QM (2011). Animal models in nonalcoholic steatohepatitis research: utility and clinical translation. *Liver Int* **31**: 440–442.
2. Yatsuji, S, Hashimoto, E, Tobari, M, Taniai, M, Tokushige, K and Shiratori, K (2009). Clinical features and outcomes of cirrhosis due to non-alcoholic steatohepatitis compared with cirrhosis caused by chronic hepatitis C. *J Gastroenterol Hepatol* **24**: 248–254.
3. Cheung, O and Sanyal, AJ (2010). Recent advances in nonalcoholic fatty liver disease. *Curr Opin Gastroenterol* **26**: 202–208.
4. Brenner, RR, Ayala, S and Garda, HA (2001). Effect of dexamethasone on the fatty acid composition of total liver microsomal lipids and phosphatidylcholine molecular species. *Lipids* **36**: 1337–1345.
5. Sher, T, Yi, HF, McBride, OW and Gonzalez, FJ (1993). cDNA cloning, chromosomal mapping, and functional characterization of the human peroxisome proliferator activated receptor. *Biochemistry* **32**: 5598–5604.
6. Kersten, S, Seydoux, J, Peters, JM, Gonzalez, FJ, Desvergne, B and Wahli, W (1999). Peroxisome proliferator-activated receptor alpha mediates the adaptive response to fasting. *J Clin Invest* **103**: 1489–1498.
7. Huang, H, McIntosh, AL, Martin, GG, Petrescu, AD, Landrock, KK, Landrock, D *et al.* (2013). Inhibitors of fatty acid synthesis induce PPAR α -regulated fatty acid β -oxidative genes: synergistic roles of L-FABP and glucose. *PPAR Res* **2013**: 865604.
8. Torra, IP, Chinetti, G, Duval, C, Fruchart, JC and Staels, B (2001). Peroxisome proliferator-activated receptors: from transcriptional control to clinical practice. *Curr Opin Lipidol* **12**: 245–254.
9. Schoonjans, K, Staels, B and Auwerx, J (1996). Role of the peroxisome proliferator-activated receptor (PPAR) in mediating the effects of fibrates and fatty acids on gene expression. *J Lipid Res* **37**: 907–925.
10. Lee, GY, Kim, NH, Zhao, ZS, Cha, BS and Kim, YS (2004). Peroxisomal-proliferator-activated receptor alpha activates transcription of the rat hepatic malonyl-CoA decarboxylase gene: a key regulation of malonyl-CoA level. *Biochem J* **378**(Pt 3): 983–990.
11. Francis, GA, Annicotte, JS and Auwerx, J (2003). PPAR-alpha effects on the heart and other vascular tissues. *Am J Physiol Heart Circ Physiol* **285**: H1–H9.
12. Mayr, C, Hemann, MT and Bartel, DP (2007). Disrupting the pairing between let-7 and Hmga2 enhances oncogenic transformation. *Science* **315**: 1576–1579.
13. Leaman, D, Chen, PY, Fak, J, Yalcin, A, Pearce, M, Unnerstall, U *et al.* (2005). Antisense-mediated depletion reveals essential and specific functions of microRNAs in Drosophila development. *Cell* **121**: 1097–1108.
14. Deng, Z, Du, WW, Fang, L, Shan, SW, Qian, J, Lin, J *et al.* (2013). The intermediate filament vimentin mediates microRNA miR-378 function in cellular self-renewal by regulating the expression of the Sox2 transcription factor. *J Biol Chem* **288**: 319–331.
15. Du, WW, Fang, L, Li, M, Yang, X, Liang, Y, Peng, C *et al.* (2013). MicroRNA miR-24 enhances tumor invasion and metastasis by targeting PTPN9 and PTPRF to promote EGF signaling. *J Cell Sci* **126**(Pt 6): 1440–1453.
16. Hatfield, SD, Shcherbata, HR, Fischer, KA, Nakahara, K, Carthew, RW and Ruohola-Baker, H (2005). Stem cell division is regulated by the microRNA pathway. *Nature* **435**: 974–978.
17. Kahai, S, Lee, SC, Lee, DY, Yang, J, Li, M, Wang, CH *et al.* (2009). MicroRNA miR-378 regulates nephronectin expression modulating osteoblast differentiation by targeting GalNT-7. *PLoS One* **4**: e7535.
18. Liu, F, Lv, Q, Du, WW, Li, H, Yang, X, Liu, D *et al.* (2013). Specificity of miR-378a-5p targeting rodent fibronectin. *Biochim Biophys Acta* **1833**: 3272–3285.
19. Poy, MN, Eliasson, L, Krutzfeldt, J, Kuwajima, S, Ma, X, Macdonald, PE *et al.* (2004). A pancreatic islet-specific microRNA regulates insulin secretion. *Nature* **432**: 226–230.
20. Triboulet, R, Mari, B, Lin, YL, Chable-Bessia, C, Bennasser, Y, Lebrigand, K *et al.* (2007). Suppression of microRNA-silencing pathway by HIV-1 during virus replication. *Science* **315**: 1579–1582.
21. Lakner, AM, Bonkovsky, HL and Schrum, LW (2011). microRNAs: fad or future of liver disease. *World J Gastroenterol* **17**: 2536–2542.
22. Esau, C, Davis, S, Murray, SF, Yu, XX, Pandey, SK, Pear, M *et al.* (2006). miR-122 regulation of lipid metabolism revealed by *in vivo* antisense targeting. *Cell Metab* **3**: 87–98.
23. Shan, SW, Fang, L, Shatseva, T, Rutnam, ZJ, Yang, X, Du, W *et al.* (2013). Mature miR-17-5p and passenger miR-17-3p induce hepatocellular carcinoma by targeting PTEN, GalNT7 and vimentin in different signal pathways. *J Cell Sci* **126**(Pt 6): 1517–1530.
24. Du, WW, Yang, W, Fang, L, Xuan, J, Li, H, Khorshidi, A *et al.* (2014). miR-17 extends mouse lifespan by inhibiting senescence signaling mediated by MKP7. *Cell Death Dis* **5**: e1355.
25. Shan, SW, Lee, DY, Deng, Z, Shatseva, T, Jeyapalan, Z, Du, WW *et al.* (2009). MicroRNA MiR-17 retards tissue growth and represses fibronectin expression. *Nat Cell Biol* **11**: 1031–1038.
26. Aoyama, T, Peters, JM, Iritani, N, Nakajima, T, Furihata, K, Hashimoto, T *et al.* (1998). Altered constitutive expression of fatty acid-metabolizing enzymes in mice lacking the peroxisome proliferator-activated receptor alpha (PPARalpha). *J Biol Chem* **273**: 5678–5684.
27. Leone, TC, Weinheimer, CJ and Kelly, DP (1999). A critical role for the peroxisome proliferator-activated receptor alpha (PPARalpha) in the cellular fasting response: the PPARalpha-null mouse as a model of fatty acid oxidation disorders. *Proc Natl Acad Sci USA* **96**: 7473–7478.
28. Peters, JM, Hennuyer, N, Staels, B, Fruchart, JC, Fievet, C, Gonzalez, FJ *et al.* (1997). Alterations in lipoprotein metabolism in peroxisome proliferator-activated receptor alpha-deficient mice. *J Biol Chem* **272**: 27307–27312.
29. Farrell, GC and Larter, CZ (2006). Nonalcoholic fatty liver disease: from steatosis to cirrhosis. *Hepatology* **43**(2 Suppl 1): S99–S112.
30. Angulo, P (2002). Nonalcoholic fatty liver disease. *N Engl J Med* **346**: 1221–1231.
31. Carmiel-Haggai, M, Cederbaum, AI and Nieto, N (2005). A high-fat diet leads to the progression of non-alcoholic fatty liver disease in obese rats. *FASEB J* **19**: 136–138.
32. Cohen, JC, Horton, JD and Hobbs, HH (2011). Human fatty liver disease: old questions and new insights. *Science* **332**: 1519–1523.
33. Yang, X, Du, WW, Li, H, Liu, F, Khorshidi, A, Rutnam, ZJ *et al.* (2013). Both mature miR-17-5p and passenger strand miR-17-3p target TIMP3 and induce prostate tumor growth and invasion. *Nucleic Acids Res* **41**: 9688–9704.
34. Fang, L, Li, H, Wang, L, Hu, J, Jin, T, Wang, J *et al.* (2014). MicroRNA-17-5p promotes chemotherapeutic drug resistance and tumour metastasis of colorectal cancer by repressing PTEN expression. *Oncotarget* **5**: 2974–2987.
35. Rutnam, ZJ, Du, WW, Yang, W, Yang, X and Yang, BB (2014). The pseudogene TUSC2P promotes TUSC2 function by binding multiple microRNAs. *Nat Commun* **5**: 2914.
36. Fang, L, Du, WW, Yang, X, Chen, K, Ghanekar, A, Levy, G *et al.* (2013). Versican 3'-untranslated region (3'-UTR) functions as a ceRNA in inducing the development of hepatocellular carcinoma by regulating miRNA activity. *FASEB J* **27**: 907–919.
37. Li, H, Chang, L, Du, WW, Gupta, S, Khorshidi, A, Sefton, M *et al.* (2014). Anti-microRNA-378a enhances wound healing process by upregulating integrin beta-3 and vimentin. *Mol Ther* **22**: 1839–1850.